# Unambiguous Proof for Berry's Phase in the Sodium Trimer: Analysis of the Transition $A^2E'' \leftarrow X^2E'$

H. von Busch, Vas Dev, H.-A. Eckel, S. Kasahara, J. Wang, and W. Demtröder
*Fachbereich Physik, Universität Kaiserslautern, D-67653 Kaiserslautern, Germany*

P. Sebald and W. Meyer
*Fachbereich Chemie, Universität Kaiserslautern, D-67653 Kaiserslautern, Germany*
(Received 29 June 1998)

Precise *ab initio* calculations of the rovibrational structures of the $A^2E''$ and $X^2E'$ electronic states of $Na_3$ prompt a new vibrational assignment of the $A \leftarrow X$ transition and provide the basis for the rotational analysis of the vibrational band $A(v_s = 1, v_b = 0, v_a = 0) \leftarrow X(0,0,0)$ by means of high-resolution optical-optical double resonance. The calculations, which use the single-surface adiabatic approach, reproduce our experimental data only if, as required by theory, a geometric phase of $\pi$ under pseudorotation around the equilateral configuration is imposed. We consider this the first verification of Berry's phase in high-resolution molecular spectroscopy. [S0031-9007(98)07707-2]

PACS numbers: 31.15.Ar, 33.15.Hp, 33.20.Kf, 33.40.+f

The sodium trimer represents a textbook example of the Jahn-Teller (JT) theorem according to which, in nonlinear conformations, electronic degeneracy by symmetry is unstable towards the symmetry-reducing modes of vibration [1]. In $Na_3$, the degeneracies which occur in some of the electronic states at equilateral geometries take on the shape of conical intersections of two adiabatic potential energy surfaces (PES).

If the JT stabilization is strong compared to the vibrational energy, the internal motion of the molecule will be confined to the lower sheet of the potential, and a single-surface adiabatic treatment should be fully adequate. Furthermore, an unusual kind of vibrational motion will arise which encircles the point of degeneracy (Fig. 1). Since theory predicts a sign change of the electronic wave function under a full cycle of this so-called pseudorotation around the conical intersection [2], the nuclear wave function must also change sign. This represents a molecular version of Berry's geometric phase [3], which here takes the value $\pi$. A short survey of earlier investigations of geometric phases in molecules can be found in a recent paper on the vibronic structure of the $Na_3$ $X$ state [4]. For reviews on Berry's phase in a more general context see, e.g., Refs. [5] and [6].

In the $Na_3$ molecule, the consequences of the geometric phase would show most obviously for a free pseudorotational (PsR) motion, namely, as a half-integer quantization of the vibrational angular momentum $j$, with levels of $A_1/A_2$ and $E$ vibronic symmetry alternating according to $2j/3$ being integer or not. Such a free case is approximately realized in the $B$ state of $Na_3$. Indeed the first, low-resolution spectra of this state were interpreted as evidence for half-integer values of $j$ [7]. However, as subsequently established both by calculations [8] and by measurements with rotational resolution [9], the $Na_3$ $B$ state exhibits only a pseudo-JT distorted nondegenerate surface with a pseudorotation that is integer quantized; i.e., the geometric phase is 0.

If pseudorotation is hindered by significant barriers, as is the case in the $X$ and $A$ states of $Na_3$, $E$ and $A$ vibronic levels appear in weakly split pairs. Since the energetic order within these pairs is reversed if the geometric phase is changed from $\pi$ to 0 [10], the different rotational fingerprints of the $E$ and $A$ vibronic partners give conclusive evidence of the actual value of Berry's phase.

The present paper treats the $A \leftarrow X$ transition of $Na_3$. Both states involved have conical potential intersections

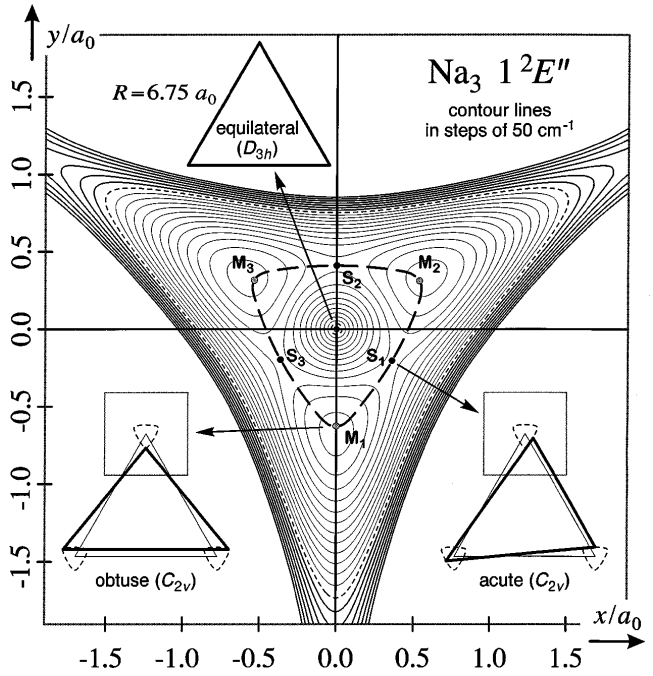


FIG. 1. Cut through the lower adiabatic PES of the electronic $A$ state of $Na_3$ for $E$ mode atomic displacements.

 0031-9007/98/81(21)/4584(4)$15.00 

at equilateral geometries. The progression of the $A$ vibrational levels to which the $X(0,0,0)$ state populated in our experiment can be excited (Fig. 2) is accompanied by significant changes in the degree to which pseudorotation is hindered by potential barriers: In the nearly rigid vibrational ground state, which is localized in the potential wells at obtuse $C_{2v}$ configurations, the coupling between the three equivalent minima only shows up as a PsR tunneling splitting (into an $E/A$ doublet) that is as small as $10^{-2}$ cm$^{-1}$. With increasing vibrational excitation, an intermediate regime follows where the vibrational levels exhibit splittings on the order of the rotational energy scale. Finally, rather delocalized vibrational states are reached in which the rotational levels of the $E/A$ vibronic components are clearly separated.

Independent experiments in Hanover [11] and in our laboratory [12] showed in fact that the rotational structures of the $X$ and $A$ vibrational *ground* states can be successfully assigned in terms of a rigid asymmetric rotor. This description, however, breaks down even for the lowest excited vibrational $A$ state, as further measurements by our group soon revealed.

Because of the large amplitude of the vibrational motion on the strongly anharmonic potentials, an assignment of the experimental spectra requires some guiding theoretical predictions. We have therefore performed calculations of rovibrational energy levels on new *ab initio* potential energy surfaces for the two states $X$ and $A$. On this basis we have been able to rovibronically assign all observed bands up to 170 cm$^{-1}$ above the $A \leftarrow X$ origin and thus to verify by experiment that a proper adiabatic treatment must indeed include a geometric phase of $\pi$.

In this paper we focus on the strongest of the higher vibrational bands; i.e., the fundamental transition $A(1,0,0) \leftarrow X(0,0,0)$ in the breathing mode. Its tunneling splitting of 1.6 cm$^{-1}$ exceeds the rotational energy spacings for smaller values of the angular momentum quantum number $N$, and it is also much larger than the uncertainties of our calculated energy levels. This band is therefore well suited for exploring the effects of Berry's phase.

*Experiment.*—Our setup has been described in detail elsewhere [12]. In short, argon gas at $p \approx 6$ bar seeded with sodium vapor at a temperature of ≈960 K expands adiabatically into vacuum through a nozzle of 70 $\mu$m diameter and 400 $\mu$m length. In this process, along with mono- and dimers and very small fractions of higher clusters, sodium trimers are formed. After passing a skimmer of 1 mm diameter at a distance of 10 mm from the nozzle, they propagate through the detection chamber as a cold supersonic molecular beam at a velocity of $1 \times 10^3$ m/s. At three interaction zones, the molecular beam is crossed perpendicularly by continuous laser beams. We use two independent single-mode dye lasers ("pump" and "probe") with a power of ≈100 mW each and one 8 W single-line (514.5 nm) $Ar^+$ "ionization" laser, which are arranged as follows: A fraction of ≈5% of the pump laser beam is utilized for monitoring laser-induced fluorescence (LIF) at a distance $d_1 = 120$ mm from the nozzle; the rest intersects the molecular beam at $d_2 = 280$ mm. At $d_3 = 380$ mm, the superimposed beams of the probe and ionization lasers are focused by a cylindrical lens to form a light sheet of ≈30 $\mu$m thickness which the molecular beam crosses in the extraction region of an ion multiplier. This zone is used for resonant two-photon ionization (RTPI).

Since the narrowly spaced rovibronic transitions of $Na_3$ show a hyperfine substructure with a width of about 2 GHz, there is usually considerable overlap, so that even at a resolution of better than 50 MHz the LIF or RTPI excitation spectra are so complicated as to presently defy direct interpretation. A solution is offered by optical-optical double resonance (OODR), a labeling technique which we implement as follows: The pump laser is fixed to a prominent peak of the LIF spectrum and is modulated by a chopper with frequency $f$. The population of both the initial and the final levels of the pump transition will be modulated accordingly, although with opposite signs. This modulation provides the label. If the RTPI signal taken downstream from the pump zone is filtered by a lock-in amplifier tuned to $f$, the only transitions observed will be those which either start from the same level as the pump transition ("primary resonances") or start from levels populated on the way from pump to probe by backfluorescence from the upper pump level ("secondary resonances"). Primary and secondary resonances will differ in sign. For

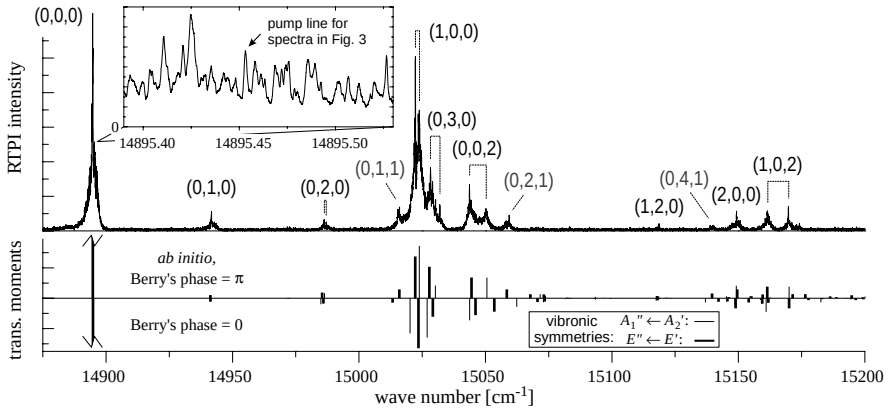


FIG. 2. Top: the $A \leftarrow X$ system of $Na_3$ and its assignment in terms of transitions $A(v_s, v_b, v_a) \leftarrow X(0,0,0)$. The brackets indicate the pseudorotational splittings. Bottom: absolute values of transition moments calculated *ab initio*.

our measurement, we put the pump on a fixed line in the $A(0,0,0) \leftarrow X(0,0,0)$ band and scanned the probe through the $A(1,0,0) \leftarrow X(0,0,0)$ band. It is difficult to find a pump line that is "clean" in the sense that it represents one (or several) hyperfine/pseudorotational component(s) of only *a single* rigid-rotor rotational transition. Even such a clean pump line must be anticipated to simultaneously deplete both pseudorotational sublevels to some degree, since we found a mixing of these doublets in $X(0,0,0)$ when doing other OODR measurements in which the pump was placed in an *excited* (and thus pseudorotationally well-separated) band. In the present case, we chose a pump line at 14895.45 $cm^{-1}$ (see the inset of Fig. 2), which from OODR in $A(0,0,0) \leftarrow X(0,0,0)$ is known to contain little intensity from asymmetric rotor transitions other than $(N_{K_a,K_c})\ 3_{2,1} \leftarrow 2_{1,1}$.

*Calculations.*—We have performed *ab initio* multireference configuration interaction (MR-CI) calculations [13], including an effective core polarization potential [14] and using a large Gaussian-type orbital (GTO) basis set with bond-center functions. The numerical potential energy surfaces have been cast in analytical form by expansions in terms of Morse-transformed internuclear distances [15] with standard deviations of $\approx 0.6$ $cm^{-1}$ for 109 calculated points. Table I collects some properties of the two PES relevant here, and Fig. 1 depicts a 2D cut through the $A$ state surface. Further details will be given elsewhere.

Rovibrational energy levels for $N \leq 4$ have been determined by variational calculations, using hyperspherical coordinates for the exact vibration-rotation Hamiltonian as well as for contracted analytical basis functions [16]. In hyperspherical coordinates, it is rather trivial to impose the geometric phase as a boundary condition on $\phi$ in a single-surface adiabatic treatment [16]. The results for $N = 0$ are included in Fig. 2 as bars, slightly shifted to match the $A \leftarrow X$ transition origin. As expected, the pseudorotational components of $E$ and $A$ vibronic symmetry reverse order upon changing the boundary condition. Comparison with experiment does give a clear preference for the correct phase $\pi$, but a definitive conclusion requires an analysis of the underlying rotational structure. Since the bars in Fig. 2 represent absolute values of the calculated *transition moments*, the experimental intensities are obviously reproduced only qualitatively. However, the calculated *vibrational energies* coincide to within a couple of $cm^{-1}$ with the observed band origins. This agreement is considerably better than that obtained only recently for the $X$ state [4]. Inspection of the wave functions reveals that the separation of the motion in the three equivalent wells is sufficient for an assignment in terms of $C_{2v}$ vibrational quantum numbers. For the correct phase $\pi$, $E$ components are lower for $v_3$ even, but higher for $v_3$ odd. We note that our assignment differs completely from that proposed by Dugourd *et al.* [17] and removes the inconsistent identification of the first excited band, which shows appreciable strength, with the transition $A(0,0,1) \leftarrow X(0,0,0)$, which has very small theoretical intensity. A more detailed account of the vibrational states will be published elsewhere.

The calculated rotational/pseudorotational (R/PsR) levels of a vibrational band are very well reproduced by an effective Hamiltonian in the $\phi$ coordinate which is readily derived from the full Hamiltonian in hyperspherical coordinates. In the case of relatively high barriers, it may be assumed that the $\phi$ space pertinent to a particular vibrational level can be spanned by three equivalent functions rotated by $2\pi/3$. This Hamiltonian then amounts to treating rotation and pseudorotation by a combination of three equivalent rotors with an angle of $2\pi/3$ between their in-plane principal axes of inertia. A least-squares fit furnishes five parameters, i.e., the three rotational constants, the potential coupling ($= 1/3$ of the tunneling splitting), and the Coriolis coupling between rotation and pseudorotation. Since the inertial defects turn out to be small, the rotational constants establish an effective $C_{2v}$ structure for each vibrational level. Table II presents the parameters of this effective Hamiltonian for three vibrational states. Note that a positive sign of $V$ reflects the energetic order $E$ below $A$.

The R/PsR levels of both vibrational ground states show a single asymmetric rotor pattern, with only very small splittings into PsR doublets of $E/A$ rovibronic symmetry. These doublets are, however, obscured by the hyperfine substructure. For the $A(1,0,0)$ state, by contrast, the vibronic $E/A$ splitting is large enough to result in two branches of rotational levels which are well separated at $N = 0$ and begin interleaving only at $N = 4$; for even higher $N$, rather irregular level patterns result which depend sensitively on the Berry phase. This interplay of rotation and pseudorotation illustrates why an earlier attempt to analyze the $A(1,0,0) \leftarrow X(0,0,0)$ band in the

TABLE I. Properties of the $Na_3$ potential surfaces.[a]

| | $X(1E')$ | | | $A(1E'')$ | | |
|---|---|---|---|---|---|---|
| | $r_{12}$ | $\alpha$ | $E$ | $r_{12}$ | $\alpha$ | $E$ |
| $C_{2v}$ (min) | 6.137 | 79.8 | −785.11 | 6.255 | 78.4 | −623.36 |
| $C_{2v}$ saddle | 6.951 | 50.0 | −579.35 | 7.037 | 50.4 | −471.70 |
| $D_{3h}$ (min) | 6.433 | 60.0 | 0.00 | 6.535 | 60.0 | 0.00 |
| $\nu_s, \nu_b, \nu_a$ | 136.0 | 49.6 | 88.5 | 128.0 | 46.5 | 77.3 |
| excit. energy | $T_{ee} = 14937, T_{00} = 14927$ [14895.769(4) [12]] | | | | | |
| ioniz. energy | $I_{ee} = 31225, I_{00} = 31252$ [31363(5) [19]] | | | | | |

[a]Distances in $a_0$, angles in degrees, energies in $cm^{-1}$.

TABLE II. Parameters of the effective R/PsR Hamiltonian.[a]

| | $vvv$ | $3V$ | $A$ | $B$ | $C$ | $c$ | $\sigma$[b] |
|---|---|---|---|---|---|---|---|
| $X$ | 000 | 0.0025 | 0.17709 | 0.08422 | 0.05680 | 0.00006 | 0.00008 |
| $A$ | 000 | 0.0167 | 0.16690 | 0.08360 | 0.05541 | 0.00026 | 0.00006 |
| $A$ | 100 | 1.5725 | 0.15514 | 0.09557 | 0.05528 | 0.02046 | 0.00648 |

[a]Potential coupling $V$; rotational constants $A$, $B$, $C$; Coriolis coupling $c$ (in $cm^{-1}$).

[b]Standard deviation for a fit of 50 ($N \leq 4$) *ab initio* levels.

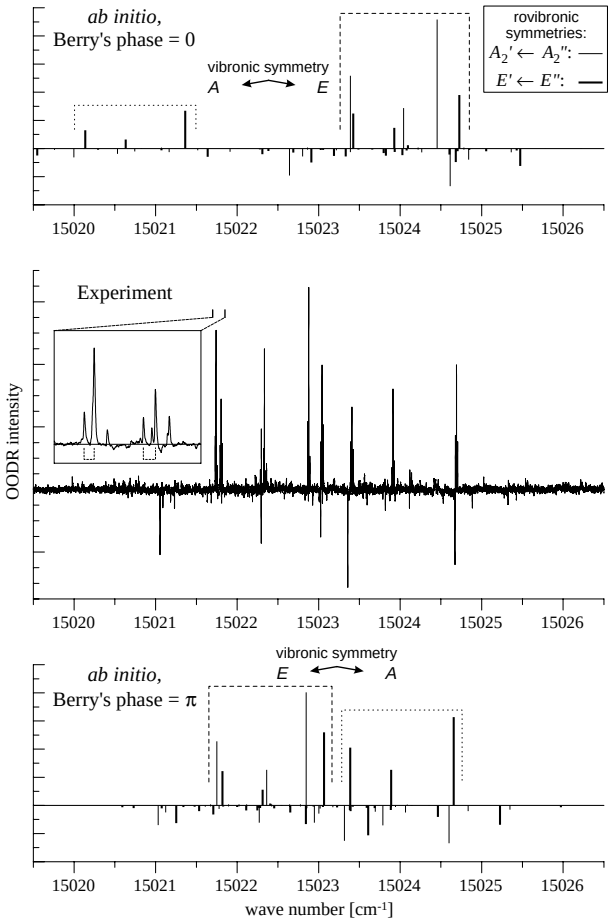


FIG. 3. OODR spectra in the band $A(1,0,0) \leftarrow X(0,0,0)$ for the pump line marked in Fig. 2. Calculations with geometric phases of 0 and $\pi$ are compared to the experimental spectrum.

simple rigid-rotor picture only applied to some OODR signals, while others could not be explained [18].

An experimental OODR spectrum obtained in $A(1,0,0) \leftarrow X(0,0,0)$, which for the given pump-line involves levels with $1 \leq N \leq 5$, is presented in Fig. 3. Shown along with it are the *ab initio* predictions for the cases with and without Berry's phase, assuming equal intensities for both pseudorotational pump-line components and an intensity fraction of 0.5 for the backfluorescence $A(0,0,0) \rightarrow X(0,0,0)$ that leads to the secondary resonances.

In the primary resonances, two different substructure patterns are found, depending on the rovibronic symmetry ($E/A$). These patterns appear to be characteristic of the given pump line, irrespective of which one of the bands is examined [except for $A(0,0,0) \leftarrow X(0,0,0)$]. In addition to the double-resonances which match those calculated for the $3_{2,1} \leftarrow 2_{1,1}$ pump transition, there are some weak primary features, as must be expected since the pump line is not completely clean. Among the secondary resonances, those of $E$-symmetry origin generally appear weaker than those of $A$ origin. This may possibly be due to a distribution of their intensity over more substructure components, most of which may be too small to clearly surpass the noise level.

Apart from the hyperfine substructure of the transitions observed, which still awaits detailed understanding, the experimental results are well reproduced by *ab initio* calculations for a geometric phase of $\pi$, while the prediction for the case without a geometric phase is clearly rejected. We stress that this conclusion is not based on a gradual deterioration of agreement but is drawn from the readily identifiable ordering of the line patterns which originate from the $E$ and $A$ vibronic components, respectively. A series of OODR spectra meanwhile obtained by us with other pump lines and in different excited vibrational bands corroborate these findings. Thus, using the example of the $Na_3$ $A \leftarrow X$ system, painstakingly optimized OODR experiments together with calculations of unprecedented accuracy have provided the first verification of Berry's phase in the alkali trimers.

[1] H. A. Jahn and E. Teller, Proc. R. Soc. London A **161**, 220 (1937).
[2] G. Herzberg and H. C. Longuet-Higgins, Discuss. Faraday Soc. **35**, 77 (1963).
[3] M. V. Berry, Proc. R. Soc. London A **392**, 45 (1984).
[4] B. Kendrick, Phys. Rev. Lett. **79**, 2431 (1997).
[5] J. W. Zwanziger, M. Koenig, and A. Pines, Annu. Rev. Phys. Chem. **41**, 601 (1990).
[6] *Geometric Phases in Physics*, edited by A. Shapere and F. Wilzcek (World Scientific, Singapore, 1989).
[7] G. Delacrétaz, E. R. Grant, R. L. Whetten, L. Wöste, and J. W. Zwanziger, Phys. Rev. Lett. **56**, 2598 (1986).
[8] R. Meiswinkel and H. Köppel, Chem. Phys. **144**, 117 (1990); F. Cocchini, T. H. Upton, and W. Andreoni, J. Chem. Phys. **88**, 6068 (1988).
[9] W. E. Ernst and S. Rakowsky, Phys. Rev. Lett. **74**, 58 (1995); Ber. Bunsenges. Phys. Chem. **99**, 441 (1995).
[10] F. S. Ham, Phys. Rev. Lett. **58**, 725 (1987).
[11] M. Meyer zur Heyde, E. Tiemann, and D. Wendlandt, Chem. Phys. Lett. **199**, 590 (1992).
[12] H.-A. Eckel, J. M. Greß, J. Biele, and W. Demtröder, J. Chem. Phys. **98**, 135 (1993).
[13] H.-J. Werner and E.-A. Reinsch, J. Chem. Phys. **76**, 3144 (1982).
[14] W. Müller, J. Flesch, and W. Meyer, J. Chem. Phys. **80**, 3297 (1984).
[15] S. Carter and W. Meyer, J. Chem. Phys. **93**, 8902 (1990).
[16] S. Carter and W. Meyer, J. Chem. Phys. **100**, 2104 (1994).
[17] Ph. Dugourd, J. Chevaleyre, J. P. Perrot, and M. Broyer, J. Chem. Phys. **93**, 2332 (1990).
[18] Th. Stoll, E. Tiemann, and D. Wendlandt, J. Mol. Spectrosc. **174**, 557 (1995).
[19] R. Thalweiser, S. Vogler, and G. Gerber, Proc. SPIE–Int. Soc. Opt. Eng. **1858**, 196 (1993).